Ultrafast magnetic flux dendrite propagation into thin superconducting films

B. Biehler, B.-U. Runge, and P. Leiderer
Physics Department, University of Konstanz, D-78457 Konstanz, Germany

R. G. Mints*
School of Physics and Astronomy, Raymond and Beverly Sackler Faculty of Exact Sciences, Tel Aviv University, Tel Aviv 69978, Israel
(Received 9 May 2005; published 20 July 2005)

We suggest a theoretical model allowing one to find analytically the velocity of a magnetic flux dendrite penetration into thin superconducting films. The key assumptions for this model are based upon experimental observations. We treat a dendrite tip motion as a propagating flux jump instability. Two different regimes of dendrite propagation are found: A fast initial stage is followed by a slow stage, which sets in as soon as a dendrite enters into the vortex-free region. The theoretical results and experimental data obtained by a magneto-optic pump-probe technique are compared and a good agreement between the calculations and measurements is found.

DOI: 10.1103/PhysRevB.72.024532 PACS number(s): 74.78.Bz, 74.25.Fy, 74.40.+k

I. INTRODUCTION

Magnetic flux penetration in type-II superconductors is successfully described by the Bean critical state model.[1] This model assumes that the slope of the flux "hills" is given by $\mu_0 j_c(T,B)$, where the critical current density $j_c(T,B)$ is a decreasing function of the temperature T and field B. Bean's critical state with its spatially nonuniform flux distribution is not at equilibrium and under certain conditions the smooth flux penetration process becomes unstable (see Ref. 2 and references therein). The spatial and temporal development of this instability depends on the sample geometry, temperature, external magnetic field, its rate of change and orientation, initial and boundary conditions, etc.

Instabilities in the critical state result in flux redistribution towards the equilibrium state (spatially homogeneous flux throughout the sample) and are accompanied by a significant heat release, which often leads to the superconductor-to-normal-transition. The basic instability observed in Bean's critical state is the flux jump instability, which was discovered already in the early experiments on superconductors with strong pinning.[2]

The basic physics of flux jumping can be easily illustrated. Assume a perturbation of temperature or flux occurring in Bean's critical state. This perturbation can be caused by an external reason or a spontaneous fluctuation arising in the system itself. The initial perturbation redistributes the magnetic flux inside the superconductor. This flux motion by itself induces an electric field which leads to dissipation, since the electric field does not only act on the Cooper pairs but also on the unpaired electrons. This additional dissipation results in an extra heating which in turn leads to an additional flux motion. This "loop" establishes a positive feedback driving the system towards the equilibrium state. The flux jumping instability exhibits itself as a suddenly appearing flux avalanche (flux jump) and heat release.[2,3]

Spatially resolved flux front patterns of Bean's critical state instability were first observed in Nb disks with thicknesses in the range of $d \approx 10^{-5}$ to 10^{-3} m by means of magneto-optic imaging.[4] Wertheimer and Gilchrist discovered a well-defined pattern of flux dendrites with a width $w \sim 10^{-3}$ m and propagation velocity v in the interval between 5 and 100 m/s.[4] The dendrites velocity depended on the disks' thickness, for smaller d a higher v was found.

The modern magneto-optic technique allowing one to investigate flux patterns with time resolution on the order of ≈ 100 ps[5,6] stimulated quite a few experimental and theoretical studies of flux front patterns arising in a process of smooth flux penetration[7] as well as in a process of critical state instability development in superconducting films in a transversal magnetic field. Different scenarios are considered resulting in a variety of flux patterns, e.g., magnetic turbulence,[8,9] kinetic flux front roughening,[10] magnetic micro avalanches,[11,12] flux dendrites,[13–17] thermomagnetic fingering,[18] bending of flux-antiflux interface,[19,20] and flux front corrugation.[21]

A wealth of recent experiments convincingly demonstrate that a propagating dendritic flux pattern driven by the flux jumping instability is a general phenomenon typical for Bean's-type critical state.[13–15,22–25] Indeed, the flux dendrites were observed under a wide variety of conditions in superconducting films of Nb,[13,14,22] $YBa_2Cu_3O_{7-\delta}$,[13,15,23] Nb_3Sn,[24] and MgB_2.[25]

It is known that dendrite propagation in thin films shows velocities up to 160 km/s,[15] i.e., these velocities are much higher than the speed of sound. This ultrafast motion of flux dendrites in thin superconducting films is a long standing and challenging problem.

In this paper we derive an equation for a dendrite tip velocity and demonstrate a good agreement between the theoretical results and experimental data for the propagation velocity of a single flux dendrite branch. The paper is organized as follows. In Sec. II we introduce the straight flux-dendrite model. The dynamics of a single flux dendrite penetration into a thin film is treated in Sec. III. In Sec. IV we compare theoretical results on the velocity of a single flux dendrite with our experimental data. Section V summarizes the obtained results.

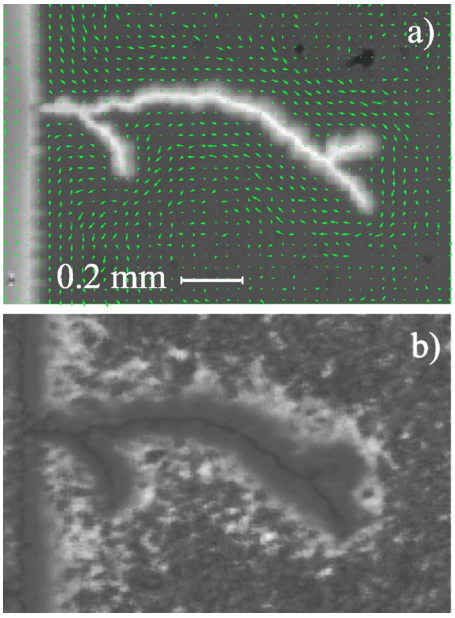

FIG. 1. (Color online) Magneto-optic images of a dendritic flux pattern in a YBCO film with the thickness $d=330$ mm subjected to a field of $B_a=15$ mT. (a) Final state (after ≈ 10 s) of a dendritic flux pattern with superimposed current distribution shown by the arrows. The length of the arrows is proportional to the local current density. (b) The absolute value of the current density is shown. The bright areas indicate high current densities.

II. STRAIGHT FLUX-DENDRITE MODEL

Dendritic flux structures which can be considered as a set of single flux branches originating from a certain area were observed in numerous experiments.[15] In the case of a dendritic structure with few branches the single branches do not affect each other. As a result penetration of flux dendrites into the sample can be treated as motion of dendrites' tips driven by the flux jumping instability with a threshold localized at the tips of the dendrites. The flux dendrite propagation generates an electric field proportional to the dendrite tip velocity. "Ignition" of the flux jumping instability has to occur in front of the tips in the area where the electric field is relatively low and the dependence of the current density on the electric field is nonlinear. This nonlinearity is important for the flux dendrite propagation process as it defines the self-consistent dendrite tip velocity.

A typical magneto-optic image of a "dilute" dendrite pattern in its final state is shown in Fig. 1(a). Superimposed are the current streamlines as determined by an inversion scheme.[26] In Fig. 1(b) the absolute value of the current density is shown. It is worth mentioning that the center of the dendrite is current free and that the current follows the dendrite branches. The current density decreases rapidly with distance from a flux dendrite.

These experimental observations allow for a straight-line flux dendrite model, which we use in our calculations. This model assumes the following.

(a) The current of a straight-line dendrite first flows parallel to the sample edge, then closely follows the contour of the dendrite branch until flowing parallel to the sample edge again as shown in Fig. 2.

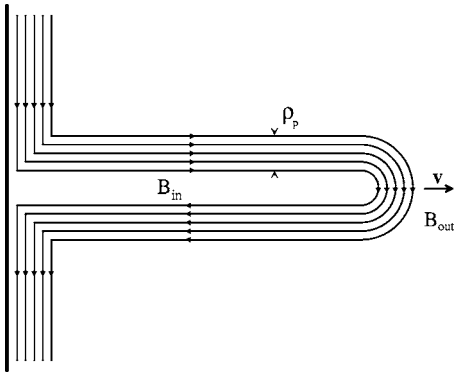

FIG. 2. Current lines for the straight-line magnetic flux dendrite. The full line to the left marks the strip edge.

(b) In the current carrying area in front of a propagating flux dendrite tip the electric field E is relatively low, the superconductor is in the flux creep regime and thus the current density j dependence on E is a power law

$$j = j_c(E/E_0)^{1/n}, \tag{1}$$

where j_c is the critical current density, and n and E_0 are the parameters characterizing the current density-electric field curve (at $E=E_0$ we have $j=j_c$).[27] It is common to define j_c as the current density at $E_0=10^{-4}$ V/m, for high-T_c superconductors $n\sim 10$ but decreases with the applied magnetic field.[28] Equation (1) yields the electric field dependent conductivity

$$\sigma(E) = \frac{dj}{dE} \approx \frac{j_c}{nE}. \tag{2}$$

Next, we denote the radius of the dendrite tip as ρ_0 and the width of the current carrying area as

$$\rho_p = B_{\text{eff}}/\mu_0 j_c, \tag{3}$$

where $B_{\text{eff}}=B_{\text{in}}-B_{\text{out}}$, B_{in} is the field inside the dendrite, and B_{out} is the field outside the tip of the dendrite.

Consider now the flux front stability at a tip of a moving flux dendrite in the framework of the model developed to treat the flux jump instability near a semicircle indentation at the sample edge.[29–31] This approach is based on the assumption that the flux jumping instability develops much faster than the magnetic flux diffusion. In the flux creep regime of low-T_c and high-T_c superconductors this assumption holds with a high accuracy.[29,30]

It follows from the general approach that the stability margin of a flux jumping instability is determined by the existence of a nontrivial solution of the thermal diffusion equation[30,31]

$$\Delta\theta - q^2\theta + \frac{nE}{\lambda}\left|\frac{\partial j_c}{\partial T}\right|\theta = 0, \tag{4}$$

where θ is the temperature perturbation, λ is the heat conductivity, E is the electric field generated by a time dependent magnetic field, the parameter q is given by

$$\tan qd = h/\lambda q, \tag{5}$$

and h is the heat transfer coefficient to the coolant. The boundary condition to Eq. (4) is $\mathbf{n}\nabla\theta=0$ at the edge of the film and $\mathbf{n}$ is the unit vector perpendicular to the edge of the film. It is clear from Eq. (4) that the flux front stability is highly sensitive to the electric field E generated by the varying magnetic field.[29–31]

III. FLUX DENDRITE TIP VELOCITY

The dendrite tip motion results in an electric field $\mathbf{E}$, which is parallel to the current density $\mathbf{j}$. We consider this field similar to the consideration of the electric field generated by a varying magnetic field at a semicircular indentation with a radius ρ_0 in a superconducting film with a straight edge.[31] This approach results in

$$E \approx \dot{B}_{\text{in}}\rho_p^2/\rho_0. \tag{6}$$

Assuming that $\rho_0 \leqslant \rho_p$ we estimate the magnetic field rate in the vicinity of a dendrite tip propagating with a velocity v as

$$\dot{B}_{\text{in}} \approx vB_{\text{eff}}/\rho_p. \tag{7}$$

Combining Eqs. (6) and (7) we find that the electric field generated at the inner edge of a moving flux dendrite tip can be estimated as

$$E \approx vB_{\text{eff}}\,\rho_p/\rho_0. \tag{8}$$

Next, we assume a high thermal boundary resistance in the films, which means that $hd \ll \lambda$. This assumption can be justified using typical values $\lambda=0.1$ W K^{-1} m^{-1}, $d=330$ nm, and $h=(700 \text{ to } 1.3\times10^3)$ W K^{-1} m^{-2}.[32–34] In this case of $hd \ll \lambda$ we find from Eq. (5) that the value of $q^2 \approx h/\lambda d$ and the stability criterion for flux jumping in thin film takes the form[31]

$$\frac{B_{\text{eff}}^2\dot{B}_{\text{in}}nd}{2\mu_0^2\rho_0 h j_c^2}\left|\frac{dj_c}{dT}\right| = 1. \tag{9}$$

Consider now the critical current density to be linear in temperature, i.e., $j_c=j_0(1-T/T_c)$. In this case we use Eq. (7) to rewrite Eq. (9) as follows:

$$v = \gamma\frac{2\mu_0^2 j_c^2 hT_c\rho_0\rho_p}{ndj_0B_{\text{eff}}^3}, \tag{10}$$

where $\gamma\sim1$ is a numerical factor and j_0 is the critical current density at $T=0$. If we assume that $\rho_0\approx\rho_p$ and use Eq. (3) then

$$v = 2\gamma\frac{hT_c}{ndB_{\text{eff}}\,j_0} = 2\gamma\frac{hT_c}{nd(B_{\text{in}}-B_{\text{out}})j_0}. \tag{11}$$

It is worth noting that the criterion (9) gives the lower limit of a dendrite tip speed. In other words, Eqs. (9)–(11) describe motion of the threshold of a local flux jumping instability. It is then obvious that a lower heat transfer to the coolant results in a lower critical state stability threshold. Therefore the instability occurs at lower electric fields and slower moving dendrite tips ($v\propto h$).

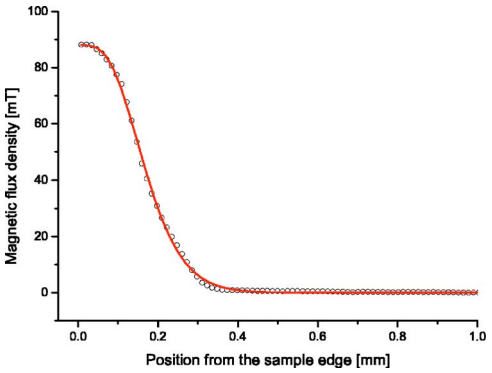

FIG. 3. (Color online) Shown is the magnetic flux distribution in our superconducting sample measured perpendicular to the edge. The measured data are shown as circles, whereas the solid line represents a least-squares fit. This fitting function given by Eq. (12) was used as $B_{\text{out}}(s)$.

IV. COMPARISON WITH EXPERIMENT

We now compare the results obtained by Eq. (11) and our experimental data. To measure the time dependent dendrite length $s=s(t)$ we used a magneto-optic single shot pump-probe setup.[15] The dendrites where nucleated at the edge of a square YBCO thin film sample by focusing one part of a single fs-laser pulse onto the film surface. The second part of the laser pulse is fed into an optical delay line and is used as the illumination source. This gives snapshots of the flux distribution after a given time. The time resolution is limited by the response time of the magneto-optical layer. A typical experiment was conducted as follows: The sample (10 mm by 10 mm YBCO film deposited on $SrTiO_3$ with a thickness of 330 nm) was zero field cooled to 10 K and a magnetic field of 17.3 mT was applied prior to the pump-probe run.

We observed two qualitatively different stages of dendrite propagation. In the first few nanoseconds we observed an extremely high velocity on the order of 160 km/s, later on this velocity decreased to a value of 18 km/s. For additional experimental details see Ref. 15. The existence of these two distinct regions of dendrite propagation can be easily understood using Eq. (11). Indeed, as long as a dendrite crosses the critical state area the field B_{out} is decreasing, therefore the value of $B_{\text{eff}}=B_{\text{in}}-B_{\text{out}}$ is increasing and consequently the velocity of the dendrite is decreasing. After the dendrite tip crosses the critical state area its velocity stays constant as the dendrite runs in a vortex-free area where B_{eff} is a constant.

The time dependence of the dendrite length $s=s(t)$ can be calculated using Eq. (11). The effective field B_{eff} is the crucial parameter for this calculation. To find B_{eff} we measured the flux distribution on the edge of the sample by using our magneto-optic setup. The data (circles) and a fit (solid line) are shown in Fig. 3. We use the function

$$B_{\text{out}}(s) = \frac{a_1}{\cosh^4(s/a_2)} + \frac{a_3}{\cosh^2(s/a_4)} \tag{12}$$

as a fitting function. The least-squares fit of Eq. (12) to the experimental data results in $a_1=295.22$ mT, $a_2=0.212$ mm, $a_3=-207.11$ mT, and $a_4=0.125$ mm, with a coefficient of

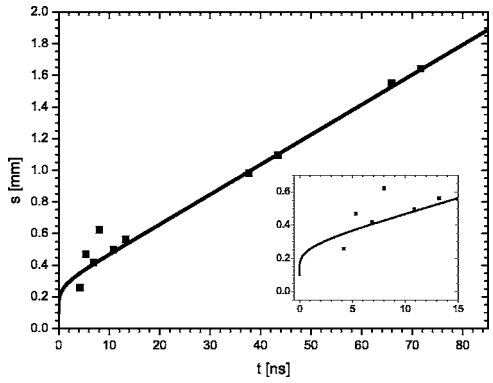

FIG. 4. The time dependence of the length of a magnetic flux dendrite, $s(t)$. The solution of Eqs. (14) and (15) with $s_0=0.1$ mm and $\alpha=1.67$ is shown by the solid line; the experimental data are shown by the solid dots (Ref. 15). The dependence $s(t)$ for the first 15 ns is shown in the inset.

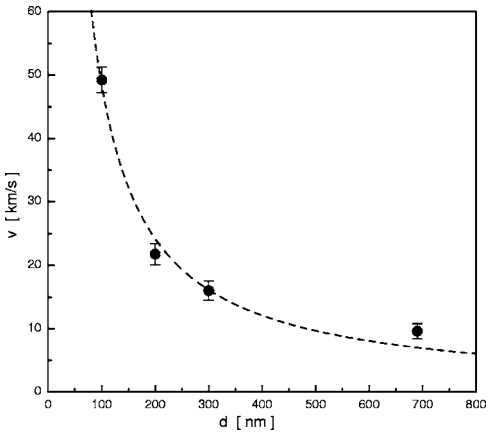

FIG. 5. The dependence of the flux dendrite velocity on the sample thickness $v(d)$. The dashed line is a fit of $v \propto 1/d$ revealing the dependence given by Eq. (11) and the solid dots are the experimental data (Ref. 35).

determination $R^2=0.9993$ and $\chi^2=0.485$, where χ^2 is the sum of the squared deviations divided by the number of used data points minus the number of parameters (degrees of freedom). Using the fitting function in Eq. (11) as $B_{\text{out}}(s)$ we obtain a differential equation for the dendrite propagation

$$\frac{ds}{dt} = \frac{\alpha}{B_{\text{in}} - B_{\text{out}}(s)}, \tag{13}$$

with $\alpha=2\gamma h T_c/ndj_0$. Based on our experimental data we assume that the field B_{in} is constant and equal to the field at the sample edge, i.e., $B_{\text{in}}=B_{\text{out}}(0)$.

The solution of Eq. (13) with the initial condition $s(0)=s_0$ takes the form

$$\mathcal{D}(s) - \mathcal{D}(s_0) = \alpha t, \tag{14}$$

where

$$\mathcal{D}(s) = (a_1 + a_2)s - \frac{a_1 a_2}{3}\left(2 + \frac{1}{\cosh^2(s/a_2)}\right)\tanh(s/a_2) - a_3 a_4 \tanh(s/a_4). \tag{15}$$

The dependence $s(t)$ following from Eqs. (14) and (15) is shown in Fig. 4 by the solid line. We use for this plot $s_0=0.1$ mm and the values $d=330$ nm, $T_c=90$ K, $j_0=9\times10^{10}$ A/m^2, $h=3\times10^3$ W K^{-1} m^{-2}, $\gamma=0.75$, and $n=8$, which result in $\alpha\approx1.67$ and $\mathcal{D}(s_0)\approx0.26$. It follows from Fig. 4 that with these reasonable assumptions we find a good agreement between experiment and theory.

To check Eq. (11) further we compare the calculated velocities with the velocities obtained from line-focus measurements.[15] In this case, a line through the center of the sample is *heated* and dendrites start to run not only at the sample edge, but perpendicular to the heated line, too. Moreover, in the line-focus experiments the heated line cuts into the Meissner phase through the sample center. Therefore dendrites originating near the center never cross the critical state region but instead penetrate into the flux-free area. In this case, as expected from Eq. (11), we do not find a regime with increased velocities, however, we find a thickness dependence.

In Fig. 5 one can see the experimentally obtained thickness dependent velocity and a fit $v\propto1/d$. One reason for the slight deviations between the theory and experiment may be that we had to use different YBCO films to obtain the data, i.e., the values for parameters like T_c or B_{eff} may vary from sample to sample.

V. SUMMARY

The main result of this study is Eq. (11). It describes the dynamics of a single flux dendrite and it was shown that a good agreement with the experimental data has been achieved.

ACKNOWLEDGMENTS

We want to thank the Kurt Lion Foundation, the Israeli Science Foundation (Grant No. 283/00-11.7), and the German Israeli Foundation (Grant No. G-721-150.14/10) for their support. Further, we want to thank H. Kinder for providing the YBCO samples.

*Email address: mints@post.tau.ac.il

[1] C. P. Bean, Rev. Mod. Phys. **36**, 31 (1964).
[2] R. G. Mints and A. L. Rakhmanov, Rev. Mod. Phys. **53**, 551 (1981).
[3] E. Altshuler and T. H. Johansen, Rev. Mod. Phys. **76**, 471 (2004).
[4] M. R. Wertheimer and J. le G. Gilchrist, J. Phys. Chem. Solids **28**, 2509 (1967).
[5] M. R. Freeman, R. R. Ruf, and R. J. Gambino, IEEE Trans. Magn. **27**, 4840 (1991).
[6] M. R. Freeman, Phys. Rev. Lett. **69**, 1691 (1992).
[7] E. H. Brandt, Rep. Prog. Phys. **58**, 1465 (1995).
[8] V. K. Vlasko-Vlasov, V. I. Nikitenko, A. A. Polyanskii, G. W. Crabtree, U. Welp, and B. W. Veal, Physica C **222**, 361 (1994).
[9] M. R. Koblishka, T. H. Johansen, M. Baziljevich, H. Hauglin, H. Bratsberg, and B. Ya. Shapiro, Europhys. Lett. **41**, 419 (1998).
[10] R. Surdeanu, R. J. Wijngaarden, E. Visser, J. M. Huijbregtse, J. Rector, B. Dam, and R. Griessen, Phys. Rev. Lett. **83**, 2054 (1999).
[11] S. Field, J. Witt, F. Nori, and X. Ling, Phys. Rev. Lett. **74**, 1206 (1995).
[12] E. R. Nowak, O. W. Taylor, L. Liu, H. M. Jaeger, and T. I. Selinder, Phys. Rev. B **55**, 11702 (1997).
[13] P. Leiderer, J. Boneberg, P. Brüll, V. Bujok, and S. Herminghaus, Phys. Rev. Lett. **71**, 2646 (1993).
[14] C. A. Durán, P. L. Gammel, R. E. Miller, and D. J. Bishop, Phys. Rev. B **52**, 75 (1995).
[15] U. Bolz, B. Biehler, D. Schmidt, B.-U. Runge, and P. Leiderer, Europhys. Lett. **64**, 517 (2003).
[16] I. Aranson, A. Gurevich, and V. Vinokur, Phys. Rev. Lett. **87**, 067003 (2001).
[17] I. S. Aranson, A. Gurevich, M. S. Welling, R. J. Wijngaarden, V. K. Vlasko-Vlasov, V. M. Vinokurl, and U. Welp, Phys. Rev. Lett. **94**, 037002 (2005).
[18] A. L. Rakhmanov, D. V. Shantsev, Y. M. Galperin, and T. H. Johansen, Phys. Rev. B **70**, 224502 (2004).
[19] F. Bass, B. Ya. Shapiro, I. Shapiro, and M. Shvartser, Phys. Rev. B **58**, 2878 (1998).
[20] L. M. Fisher, A. Bobyl, T. H. Johansen, A. L. Rakhmanov, V. A. Yampol'skii, A. V. Bondarenko, and M. A. Obolenskii, Phys. Rev. Lett. **92**, 037002 (2004).
[21] F. Bass, B. Ya. Shapiro, and M. Shvartser, Phys. Rev. Lett. **80**, 2441 (1998).
[22] V. Bujok, P. Brüll, J. Boneberg, S. Herminghaus, and P. Leiderer, Appl. Phys. Lett. **63**, 412 (1993).
[23] U. Bolz, D. Schmidt, B. Biehler, B.-U. Runge, R. G. Mints, K. Numssen, H. Kinder, and P. Leiderer, Physica C **388**, 715 (2003).
[24] I. A. Rudnev, S. V. Antonenko, D. V. Shantsev, T. H. Johansen, and A. E. Primenko, Cryogenics **43**, 663 (2003).
[25] T. H. Johansen, M. Baziljevich, D. V. Shantsev, P. E. Goa, Y. M. Galperin, W. N. Kang, H. J. Kim, E. M. Choi, M.-S. Kim, and S. I. Lee, Europhys. Lett. **59**, 599 (2002).
[26] R. J. Wijngarden, K. Heeck, H. J. W. Spoelder, R. Surdeanu, and R. Griessen, Physica C **295**, 177 (1998).
[27] See, A. Gurevich and H. Küpfer, Phys. Rev. B **48**, 6477 (1993), and references therein.
[28] J. W. Ekin, Appl. Phys. Lett. **55**, 905 (1989).
[29] R. G. Mints and A. L. Rakhmanov, J. Phys. D **15**, 2297 (1982).
[30] R. G. Mints, Phys. Rev. B **53**, 12311 (1996).
[31] R. G. Mints and E. H. Brandt, Phys. Rev. B **54**, 12421 (1996).
[32] J. L. Cohn, E. F. Skelton, S. A. Wolf, J. Z. Liu, and R. N. Shelton, Phys. Rev. B **45**, 13144 (1992).
[33] M. Nahum, S. Verghese, P. L. Richards, and K. Char, Appl. Phys. Lett. **59**, 2034 (1991).
[34] E. H. Brandt, M. V. Indenbom, and A. Forkl, Europhys. Lett. **22**, 735 (1993).
[35] U. Bolz, Ph.D. thesis, Konstanz, 2002, p. 96.